12

BIOMECHANICS RESEARCH: Experimental and Computational,
Proceedings of the Twenty Sixth International Workshop.

A Finite Element-Based Study of Pylon Fracture

R. E. Tannous, X. A. Zhang, and F. A. Bandak

ABSTRACT

A finite element model is utilized to analyze stress distributions in the tibial plafond. This preliminary effort is aimed at exploring the mechanism of pylon fracture in the ankle joint. The FE model is based on a previously developed three-dimensional finite element model of the human lower extremity. It consists of the tibia, fibula, talus, and interosseous membrane. Several simulations are conducted with different talar pre-orientation: neutral, dorsiflexion/plantarflexion, inversion/eversion, and internal/external rotation. Initial results indicate that tibial plafond localization is dependent on contact area between the talus and the distal tibia. Talar pre-inversion had the most significant effect due to the "knife edge" contact area. It produced the highest maximum principal strain value and localized on the surface of the tibial plafond. Plantar-flexion pre-orientation yielded the highest peak tibial axial forces. Initial observations showed that predicting pylon fracture from tibial forces alone is difficult.

INTRODUCTION

The occurrences of lower extremity injuries are second only to head injuries in car crashes (Pattimore et al., 1991, States, 1986). Crandall et al. (1998) examined 1988-1997 United States crash data from the National Accident Sampling System (NASS) for drivers and front seat passengers involved in car crashes with lower leg trauma severity of AIS≥2. They found that regardless of the restraint system, the lower limb is one of the most frequently injured body regions along with the head/face. This finding is also confirmed by Pattimore et al. (1991), Morgan et al. (1991). Pattimore looked at the United Kingdom Cooperative Crash Injury Study (CCIS) database and found that 37% of front seat occupants sustained lower leg trauma of AIS≥2. Morgan et. al. analyzed NASS cases between 1980-1987 for front seat occupants and concluded that 26% of AIS≥2 are lower extremity injuries.

Injury to the ankle joint can lead to serious consequences. Pylon (french, for "pestle") fracture is one of the most severe form of lower leg injury. It was first introduced by Destot in 1911 to describe these compression injuries observed at the distal end of the tibia. He likened the shape of the tibial metaphysis to that of a pharmacist's pestle, coining the term "pylon" for this anatomic structure (Ruedi et al. , 1993). Another term for this horizontal tibial articular surface is "plafond" (French , for "ceiling"). The main features of a pylon fracture are the following (Figure 1): 1) an intra-articular metaphyseal fracture of the distal tibia, 2) extension through the dome of the plafond, 3) fracture of the medial malleolus, 4) fracture of the anterior margin of the tibia, and 5) transverse fracture of the posterior tibial surface (Mainwaring, 1988; Bourne, 1989; Ayeni, 1989).

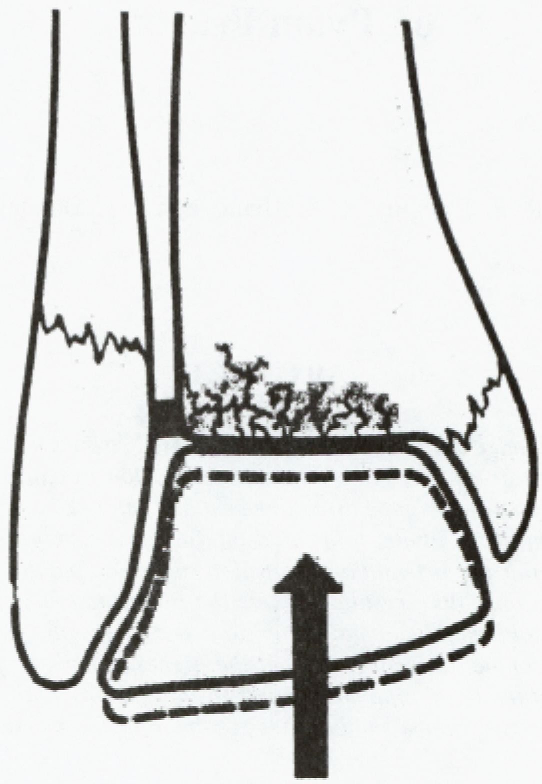

Figure 1. Schematic of a typical pylon fracture

Pylon fractures lead to long-term disability and permanent impairment. Levine (1986) determined that pylon fractures have the poorest prognosis. These fractures are difficult to treat and have a high incidence of poor results. The occurrence of pylon fractures in automotive crash environment has been examined by Taylor et al. (1997). The authors looked at the CCIS database from 1983-1996 and examined 1,112 injuries below the knee. They reported that 11.6% of all the cases sustained pylon fractures. The exact injury mechanism is still unclear, however, it is generally believed that axial compressive forces are the primary suspects. It is conjectured that vertical forces would drive the talus into the distal tibia due to intrusion or pedal interaction. In some cases, the fibula might fracture, then it is thought that rotational shear forces are involved.

It is believed that computer models along with experimental data can provide essential information on these injury mechanisms. In this paper, a previously developed and validated three-dimensional finite element model of the human ankle/foot complex was utilized to examine the mechanisms of pylon fracture (Tannous et al., 1996). To observe tibial plafond localization, a component model was extracted from the full 3D model. It contained tibia, fibula, talus, and interosseous membrane. The following is a description of the experimental work available in the literature dealing with the reproduction of pylon fracture in cadaveric specimen. Subsequently, a discussion of preliminary computational results produced by the model is presented.

PYLON FRACTURES IN CADAVERS

Several test laboratories attempted to recreate pylon fractures using cadaveric specimen. The following is a description of the various test setups employed, along with a synopsis of the results.

MCW: At the Medical College of Wisconsin (MCW), the lower limb specimen was disarticulated at the knee joint, such that the entire lower extremity distal to the knee joint remained intact. The proximal tibia was rigidly fixed in PMMA. Steinmann pins were passed transversely through the tibia complex to achieve rigid fixation. The specimen was fixed to the mini-sled (Figure 2.). The equipment consisted of two stainless steel rails rigidly attached to a steel frame. Four linear ball-bearings formed the interface between the rails and the cart assembly which were used to connect the specimen to the mini-sled. The plantar aspect of the foot was loaded axially by the pendulum impactor. A rubber pad was used in front of the impactor. A total of 28 impacts were conducted in this study. There were 13 fractures reported out of which: 2 of the talus, 8 of the calcaneus, 3 intra-articular fracture of the distal tibia (pylon fracture), 1 distal tibia-fibula, 1 of tibia. It seems that calcaneal fracture is the most frequent fracture mode. The authors demonstrated that tibial force seemed to correlate the best with injury (Yoganandan et. al., 1995; 1996). The value of the tibial axial force that produce fracture was suggested to be around 8 kN.

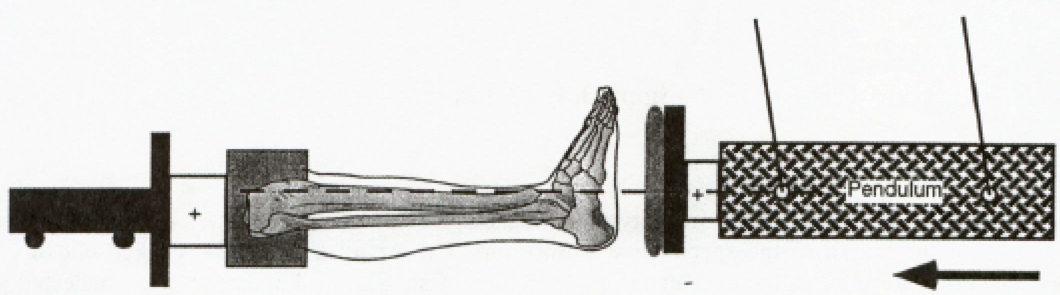

Figure 2. MCW test set-up.

UVA: At the University of Virginia (UVA), the test apparatus consisted of a contact pad, transfer piston, positioning brackets, and a foot plate which was constrained to move longitudinally. The positioning brackets allowed initial positioning of the foot and ankle complex about the flexion and xversion axes (Figure 3.). The specimen is obtained by cutting at the midshaft of the femur. All knee ligaments and leg musculature were intact. A harness was placed over the knee which was attached to a spring via a block and tackle assembly which could be adjusted to provide an initial pre-load. Among the 50 human subjects tested, 1 sustained a pylon fracture, 5 sustained calcaneal fractures, 2 sustained talar fractures, and 2 sustained ligaments tear. Resultant ankle angular velocity and the initial position of the foot had considerable influence on the injury outcome. Risk functions using a linear combination of the foot contact force or contact force onset rate, initial dorsiflexion angle, and the resultant ankle angular velocity were found to be the best predictors of injury with $p=0.0001$. Initial eversion angle has no effect on injury outcome. Forces and moments measured at the tibia and peak ankle rotations were poor predictors of injury. The tibia Index was also a poor predictor of injury.

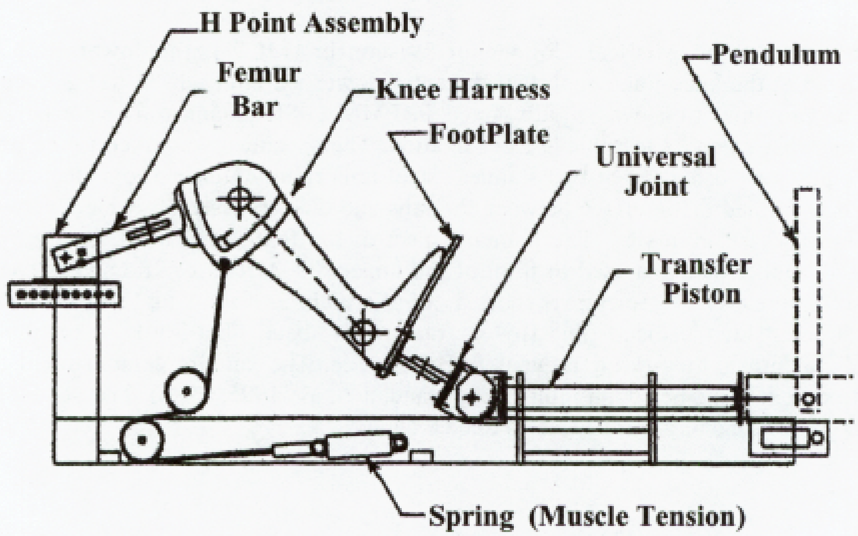

Figure 3. UVA test set-up.

WSU: At Wayne State University (WSU), the specimen were cut at the proximal end of the tibia so that the length of the specimen was 300 mm. The Achilles tendon was taken out of each specimen and placed into a tendon catcher made of steel mesh. The tendon catcher was connected to a pulley mechanism which applied a 2 kN of tensile force on the tendon without rupturing the tissue. This was done to simulate the muscular contraction of the muscles during braking. The proximal end was rigidly potted, and an 18 Kg pendulum was used to reproduce an intrusion type impact on the forefoot. It had a half an inch of ensolite padding (Figure 4.). A total of 16 specimen were tested. There were 5 of them which sustained pylon fractures. 10 specimen had calcaneal fractures, and one had no injury. The authors suggested a failure load for the tibia to be around 8 kN.

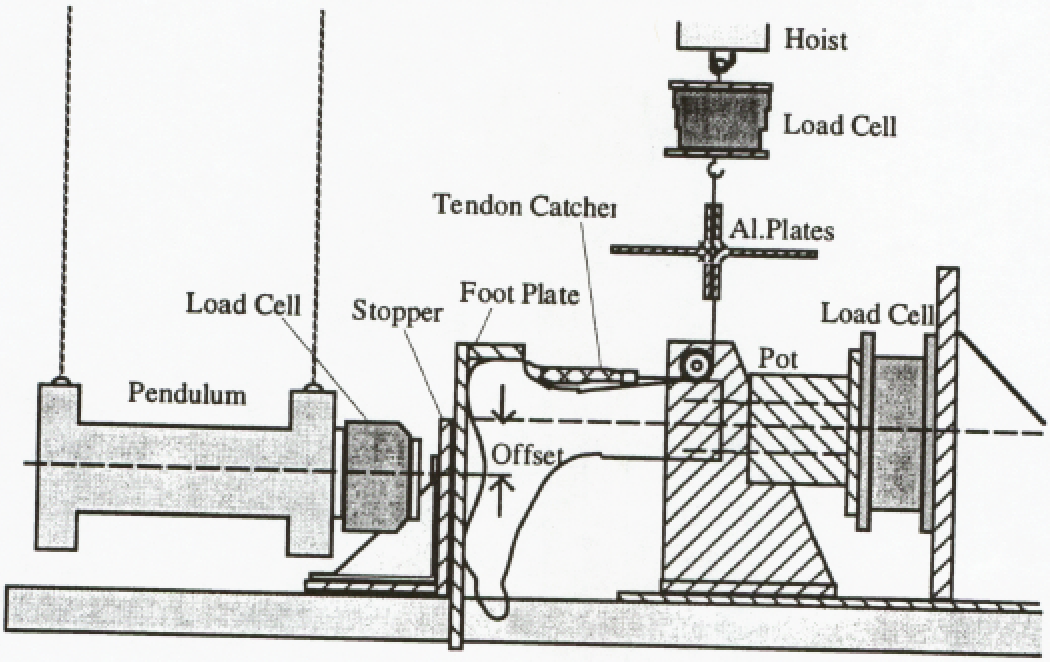

Figure 4. WSU test set-up.

In summary, it is noticed that pylon fracture is hard to reproduce in experimental settings. Calcaneal fractures seem to be the dominant mode of fracture. It is suggested from WSU's experiments that the tensile force generated in the Achilles tendon produces a compressive pre-load on the tibia combined with an impulsive external force would lead to pylon fracture. Finally, it seems that there is a consensus among researchers that an axial tibial force of around 8 kN is sufficient enough to produce fracture in the ankle joint.

MATERIALS AND METHODS

A three-dimensional finite element model of the human lower extremity is shown in Figure 5. This model was previously developed and examined under axial impact loading (Tannous et al. 1996). The model corresponds to the skeletal system of an average human foot, accurately describing the geometry of all bones of the foot and ankle. Fibula, tibia, calcaneus, talus, interosseous membrane, and the plantar soft tissue were modelled by a deformable hexagonal solid elements. Ankle ligaments, and retinacula were modelled by a deformable membrane elements. The Achilles tendon was modelled by a one-dimensional truss element. The remaining foot bones were modelled as rigid bodies. Bone interactions were controlled using contact interfaces and the ligament attachments. Thus, slide surfaces were identified between the tibia, talus, fibula, calcaneus, medial and lateral malleoli. The resulting model contains 21256 nodes with 16596 elements out of which 33% were part of the rigid body components. Preliminary results indicated reasonable overall mass and stiffness distribution and demonstrated the model capability of reproducing the experimental input/output responses under low impact velocity. However, the lack of incorporation of a material model with a failure criteria for the bone poses a limitation in the response at speeds higher than 10 mph..

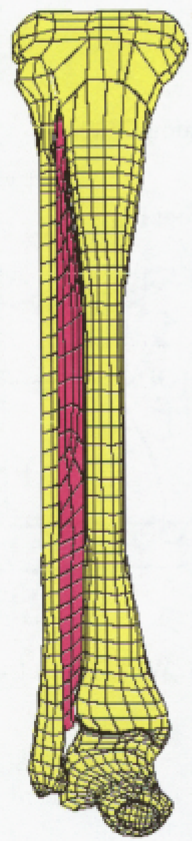

Figure 5. Frontal view of the Three-Dimensional Finite Element Component Model of the Human Ankle.

As a preliminary effort to explore pylon fracture mechanism, a component model was extracted from the existing three-dimensional FEM. This approach is explained by the following reasons: 1) Observe tibial plafond localization, 2) study the effect of talar position on energy localization in the tibial plafond, and 3) save on computational time. The component model included the tibia, fibula, talus, and interosseous tissue. It had 3,452 solid elements, and was run on LS-DYNA3D version 940 (Livermore Software Technology Corp, CA), an explicit non-linear dynamic finite element code.

A 20 ms triangular pulse was applied to the talus with an amplitude that produced an 8 kN axial tibial force. This is the reported tibial force level that caused fracture in experiments. The proximal tibia/fibula had a fixed end condition. A total of 19 simulations were ran. They correspond to seven initial condition of the talus with respect to the tibia: neutral, dorsiflexion/plantarflexion, eversion/inversion, and internal/external rotation. Each non-neutral case was simulated with three different talar angle of: 2°, 5°, and 10°.

RESULTS

Table 1. shows a comparison of tibial axial forces between the different simulations. It is clear that the axial force is dependent on talar orientation. The plantarflexion case (5°) yielded the highest tibial force value of 3900 Lbs. The dorsiflexion case (5°) produced the lowest tibial force observed in all simulations (500 Lbs). This fact can be related to the effective contact area between the talus and the tibial plafond. In the plantarflexion, the contact area between the two bones is relatively wider when compared to the dorsiflexion case. This wider area could lead to a certain load path which allows maximum transmission of axial force between the talus and the tibia.

Table 1. Tibial axial forces corresponding to the different pre-orientation position of the talus.

Pre-orientation	Tibial Force (Lbs)
Neutral	2000.0
Dorsiflexion	500.0
Plantarflexion	3900.0
Internal Rotation	850.0
External Rotation	760.0
Eversion	930.0
Inversion	1500.0

Table 2. show the maximum principal and shear strain values computed from the model for the tibial plafond for all the cases. It is noticed that the values for both parameters increases with the talar angle of orientation. In addition, for the various angles, the inversion initial condition resulted in the highest values for the maximum principal and shear strain followed by the neutral, plantarflexion, internal rotation, eversion, and dorsiflexion cases.

Table 2. Maximum principal and shear strain of the tibial plafond for all cases at 5° talar orientation.

Pre-orientation	Maximum Shear Strain	Maximum Principal Strain
Neutral	2.17e-3	3.15e-3
Dorsiflexion	1.52e-3	2.50e-3
Plantarflexion	2.03e-4	3.01e-3
Internal Rotation	1.87e-3	2.93e-3
External Rotation	1.611e-3	2.51e-3
Eversion	1.68e-3	2.88e-3
Inversion	2.54e-3	3.31e-3

The spatial distribution of maximum principal strain of the tibial plafond for the various simulations is presented in Figure 6. They correspond for the 5° talar angle pre-orientation for the different talar position. These values occurred at the peak input time of 10 ms. It is clear that the pre-inversion orientation lead to a major localization on the tibial plafond followed by neutral, plantarflexion, internal rotation, eversion, and dorsiflexion. The 10°, and 15° simulations produce similar spatial time series patterns of the maximum principal strain, with the same ordering as the 5° run. Again, the pre-inversion orientation lead to a distinct tibial plafond localization. However, as expected the value for the maximum principal strain increased with the increased angle of rotation.

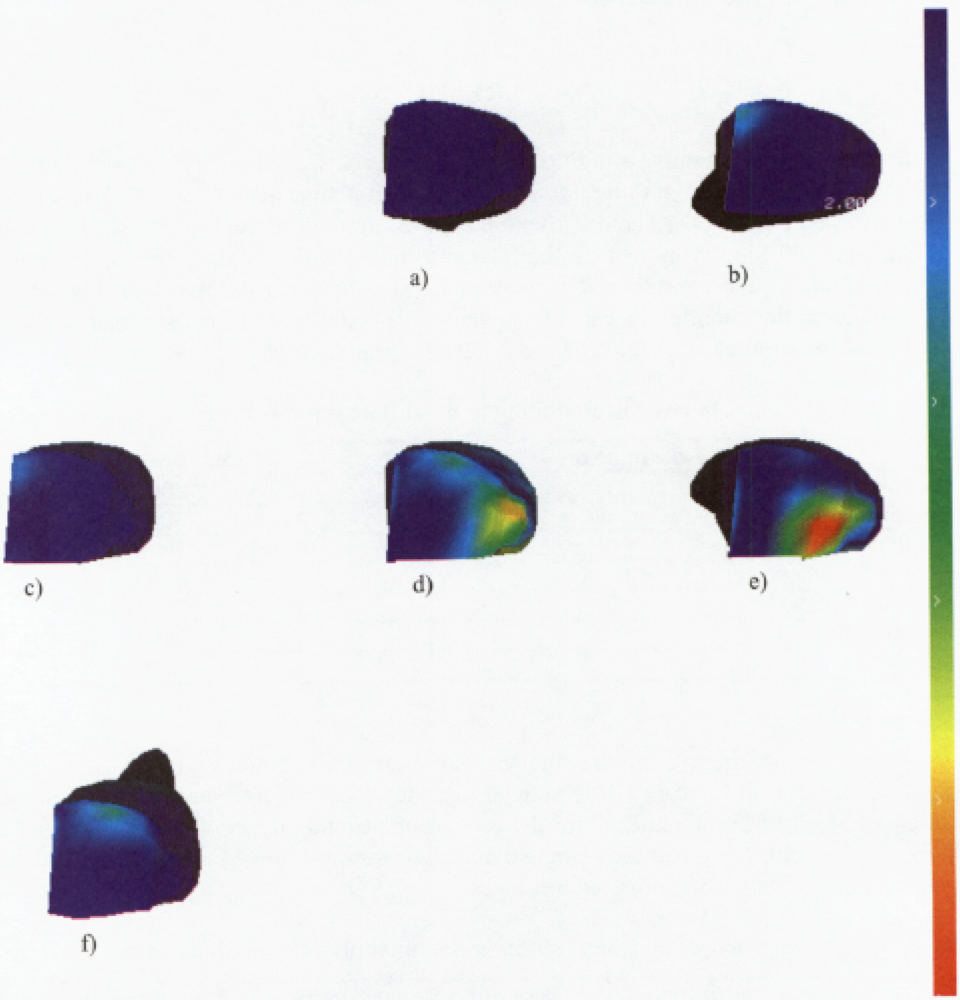

Figure 6. Spatial distribution of the maximum principal strain in the tibial plafond corresponding to different talar pre-orientation: a) dorsiflexion, b) internal rotation, c) eversion, d) neutral, e) inversion, and f) plantarflexion.

CONCLUSIONS

1. The axial force is dependent on talar orientation. The plantarflexion case produced the highest value of tibial force due to maximum contact area between the talus and tibial plafond.

2. Tibial plafond localization is dependent on contact area . The pre-inversion had the most significant due to the "knife-edge contact are" effect.

3. Predicting pylon fracture from tibial forces alone is difficult. Initial talar pre-orientation should be looked at as a major factor in producing pylon fracture in the ankle joint.

ACKNOWLEDGEMENTS

The authors appreciate information from and discussions with staff from the various laboratories conducting lower extremities experiments. Namely, J. Crandall and the UVA team, N. Yoganandan and F. Pintar at MCW, and Y. Kitagawa at WSU.

REFERENCES

Ayeni, J.P., "Pylon Fractures of the Tibia: a Study Based on 19 Cases". Injury, Vol 19., pp 109-114, (1988).

Bourne, R. B., "Pylon Fractures of the Distal Tibia." Clinical Orthopedic, Vol. 240, pp 42-46, (1989).

Kitagawa, Y., Ichikawa, H., King, A.I., Levine, R.S. "A Severe Ankle and Foot Injury in Frontal Crashes and Its Mechanicsm." Proc. of 42nd Stapp Car Crash Conference, pp. 1-12, (1998).

Mainwaring, B. L "Pylon Fractures of the Ankle: a Distinct Clinical and Radiologic Entity." Radiology, Vol. 168, No. 1, (1988).

Pattimore, D., Ward, E., Thomas, P., Bradford, M. "The Nature and Cause of Lower Limb Injuries in Car Crashes." Proc. 35th Stapp Car Crash Conference, (1991).

Ruedi, R.T., Allgower, V.T., "The Operative Treatment of Intra-Articular Fractures of the Lower End of the Tibia". Clinical Orthopedics, Vol. 138, pp. 105-110, (1993)

Tannous, R.E., F.A. Bandak, T.G. Toridis, and R.H. Eppinger, "A Three Dimensional Finite Element Model of the Human Ankle: Development and Preliminary Application to Axial Impulsive Loading." Proc. 40th Stapp Car Crash Conference, (1996).

Yoganandan, N., Pintar, F.A., Boyton, M., and Sances, J.A., " Biomechanics of Foot and Ankle Fractures." Proc. Oo the International Conference on Pelvic and Lower Extremity Injuries, pp. 201-209, (1995).

Yoganandan, N., Pintar, F.A., Boyton, M., Begeman, P., Prasad, P., "Dynamic Axial Tolerance of the Human Foot-Ankle Complex." Proc. of 40th Stapp Car Crash Conference, pp. 207-218, (1996).